ISSN 0020-4412, Instruments and Experimental Techniques, 2024, Vol. 67, No. 1, pp. 143–152. © Pleiades Publishing, Ltd., 2024.

PHYSICAL INSTRUMENTS FOR ECOLOGY, MEDICINE, AND BIOLOGY

γ-Ray Detection with the TAIGA-IACT Installation in the Stereo Mode of Observation

P. A. Volchugov[a,b,*], I. I. Astapov[d], P. A. Bez''yazykov[b], E. A. Bonvech[a], A. N. Borodin[d], N. M. Budnev[b], A. V. Bulan[a], A. Vaidyanatan[e], N. V. Volkov[i], D. M. Voronin[f], A. R. Gafarov[b], E. O. Gres'[b], O. A. Gres'[b], T. I. Gres'[b], O. G. Grishin[b], A. Yu. Garmash[e,h], V. M. Grebenyuk[d,j], A. A. Grinyuk[d], A. N. Dyachok[b], D. P. Zhurov[b], A. V. Zagorodnikov[b], A. D. Ivanova[b], A. L. Ivanova[b,e], M. A. Ilyushin[b], N. N. Kalmykov[a], V. V. Kindin[c], S. N. Kiryukhin[b], R. P. Kokoulin[b], N. I. Kolosov[b], K. G. Kompaniets[c], E. E. Korosteleva[a], V. A. Kozhin[a], E. A. Kravchenko[e,h], A. P. Kryukov[a], L. A. Kuz'michev[a], A. K'yavassa[k], A. A. Lagutin[i], M. V. Lavrova[d], Yu. E. Lemeshev[b], B. K. Lubsandorzhiev[f], N. B. Lubsandorzhiev[a], S. D. Malakhov[b], R. R. Mirgazov[b], R. D. Monkhoev[b], E. A. Okuneva[a], E. A. Osipova[a], A. D. Panov[a], A. L. Pakhorukov[b], A. Pan[c], L. V. Pan'kov[b], A. A. Petrukhin[c], D. A. Podgrudkov[a], E. G. Popova[a], E. B. Postnikov[a], V. V. Prosin[a], V. S. Ptuskin[g], A. A. Pushnin[b], A. Yu. Razumov[a], R. I. Raikin[i], G. I. Rubtsov[f], E. V. Ryabov[b], V. S. Samoliga[b], I. Satyshev[d], L. G. Sveshnikova[a], A. A. Silaev[a], A. A. Silaev (Jr.)[a], A. Yu. Sidorenkov[f], A. V. Skurikhin[a], A. V. Sokolov[e,h], V. A. Tabolenko[b], A. B. Tanaev[b], M. Yu. Ternovoi[b], L. G. Tkachev[d,j], N. A. Ushakov[f], D. V. Chernov[a], and I. I. Yashin[d]

[a]*Skobeltsyn Institute of Nuclear Physics, Moscow State University, Moscow, 119234 Russia*
[b]*Institute of Applied Physics, Irkutsk State University, Irkutsk, 664003 Russia*
[c]*National Research Nuclear University MEPhI (Moscow Engineering Physics Institute), Moscow, 115409 Russia*
[d]*Joint Institute for Nuclear Research, Dubna, Moscow oblast, 141980 Russia*
[e]*Novosibirsk State University, Novosibirsk, 630090 Russia*
[f]*Institute for Nuclear Research, Russian Academy of Sciences, Moscow, 117312 Russia*
[g]*Pushkov Institute of Terrestrial Magnetism, Ionosphere, and Radio Wave Propagation, Russian Academy of Sciences, Troitsk, Moscow, 108840 Russia*
[h]*Budker Institute of Nuclear Physics, Siberian Branch, Russian Academy of Sciences, Novosibirsk, 630090 Russia*
[i]*Altai State University, Barnaul, Altai krai, 656049 Russia*
[j]*Dubna State University, Dubna, Moscow oblast, 141980 Russia*
[k]*National Institute for Nuclear Physics (INFN), Torino, 10124 Italy*
**e-mail: pvol4@ya.ru*

Received April 21, 2023; revised June 9, 2023; accepted July 2, 2023

Abstract—The paper is devoted to the modeling and analysis of data detected by the TAIGA-IACT installation in the stereo mode. Five Imaging Atmospheric Cherenkov Telescopes (IACT) with a viewing angle of 9.6° are expected to be included in the installation. Today there are three telescopes spaced far apart (from 320 to 500 m) in the installation. The effective area of the installation is as large as 0.6 km^2; therefore, it is possible to conduct statistically significant measurements of weak γ-ray sources in the energy range above 10 TeV over a reasonable observation time (300–400 h). The Monte Carlo procedure for simulating the hadrons and γ-rays detected by the telescopes is described as is the procedure for reconstructing the parameters of extensive air showers, such as the arrival direction of an event, the axis position, the depth of the maximum of shower development ($X_{\max}$), and the primary-particle energy. In order to solve the problem of γ-hadron separation, the criteria for selecting γ-rays detected in the stereo mode have been optimized and the effective area of the installation has been calculated.

DOI: 10.1134/S0020441224700106

1. INTRODUCTION

Research in the field of γ-ray astronomy is one of the main channels for obtaining information about high-energy processes occurring in both Galactic and extragalactic objects. In particular, γ-ray astronomical observations in the energy range above 10 TeV can answer the question of the nature of cosmic rays in the knee region (3 × 10^{15} eV). Over the past 3 years, γ-rays with energies above 100 TeV have been detected for the first time from the Crab Nebula source and other galactic sources [1, 2]. This adds interest to the hadron mechanisms of generation of high-energy γ-rays [3]. Thus, such high-energy γ-rays have been detected only by high-altitude observatories that measure charged particles of extensive air showers (EAS) [1, 2, 4] generated by these particles in the Earth's atmosphere. In this regard, it seems important to reconstruct the energy spectrum of γ-rays from these sources by measuring EAS, e.g., based on the detection of Cherenkov radiation of showers.

The Tunka Astrophysical Complex, located in the Tunka Valley (Republic of Buryatia, Russia), was created to study cosmic rays by detecting Cherenkov radiation from EAS. The research was started in 1993. The first installation included only four optical detectors; nevertheless, it allowed obtaining a cosmic-ray spectrum in the knee region (3×10^{15} eV). The complex was further developed by deploying a number of prototype installations, on which the technique for reconstructing EAS parameters was tested [5]. As a result, the Tunka-133 installation has been constructed [6].

Tunka-133 began data acquisition in 2009. Currently, the installation includes 175 optical modules spread over an area of 3 km^2. Based on observations over two seasons (2009–2011), a spectrum has been obtained in the energy range of 10^{15}–10^{18} eV, and its complex structure, which had not been observed before, was subsequently confirmed by measurements of other observatories [7].

The successes of Tunka-133 led to the construction of the Tunka-Grande [8] and Tunka-REX [9] installations on the territory of the observatory with the aim of detecting cosmic rays with energies above 10 PeV and finalized in the creation of the TAIGA γ-ray observatory (Tunka Advanced Instrument for cosmic ray physics and γ-ray Astronomy) on the basis of the Tunka Astrophysical Complex [10].

The TAIGA γ-ray observatory is the northernmost observatory (51.810°, 103.067°) for detecting γ-rays in the region of very high energies (>1 TeV) and is used for long-term observations of sources with high declinations.

The uniqueness of the observatory lies in the joint use of Cherenkov detectors of different types. In addition to the installations listed above, imaging atmospheric Cherenkov telescopes (IACTs) of the TAIGA-IACT (Imaging Atmospheric Cherenkov Telescope), as well as a array of wide-angle TAIGA-HiSCORE (High Sensitivity Cosmic ORigin Explorer) detectors (Fig. 1), are used to detect EAS induced by primary high-energy particles [11]. Due to the high density of the TAIGA-HiSCORE installation, which includes 120 optical modules at a distance of 106 m from each other, the EAS energy and direction of arrival can be determined with high accuracy: 0.4°–0.5° for events with 4–5 triggered stations and ~0.1° for events with more than ten triggered stations [12, 13]. The IACTs are used in the TAIGA complex to select showers induced by γ rays. Telescopes form an image of the angular distribution of EAS light, based on of which the particle type (hadron/γ) can be determined. The IACTs are capable of detecting EAS from a distance of up to 600 m, which allows them to be placed at a sufficiently large distance from each other.

Thus, the combined use of a grid of 120 TAIGA-HiSCORE detectors and five TAIGA-IACT imaging atmospheric Cherenkov telescopes make it possible to determine the type of detected particles, their energy, and the direction of arrival. The energy threshold for the joint operation of the installations is 40 TeV. At the same time, the area covered by the installation turns out to be significantly larger compared to classic IACT stereo systems, such as HESS [14], MAGIC [15], and VERITAS [16]. The work is currently underway on designing the Cherenkov Telescope Array (CTA) γ-ray observatory aimed at research in the range of very high energies (from 20 GeV to 300 TeV) [17]. It is expected that an array of more than 100 IACTs of different types will be used in the CTA observatories located in the southern and northern hemispheres to collect significant statistics in this energy range. This is quite a challenge, both in terms of setting up the observatory and maintaining it. It is assumed that, in the final configuration, the areas covered by the southern and northern CTA observatories will be approximately 4 and 1 km^2, respectively [18].

Although the TAIGA-IACT and TAIGA-HiSCORE detectors can be jointly used in the energy range of >40 TeV, research in the field of lower energies using TAIGA instruments is also possible and is a matter of great interest to modern astrophysics. In particular, there are a number of γ-ray sources whose spectrum has been measured to ~10 TeV and now requires clarification [19, 20]. The study of the lower-energy region (>1 TeV) is possible if separate TAIGA-IACT telescopes are used (the mono mode of observations). However, the accuracy in reconstructing the EAS parameters at this approach is not too high. In particular, the energy resolution of events detected in the mono mode is 30–40% [21]. In the energy range above 8 TeV, EAS from primary γ-rays can be detected by several telescopes of the installation simultaneously (stereo mode), which leads to a significant improvement in the accuracy of reconstructing the parameters of a primary particle. Thus, the energy resolution of events recorded in the stereo mode of the TAIGA-IACT operation is approximately 10%. In this regard, the main purpose of this work is to investigate the possibility of detecting γ-rays by imaging atmospheric Cherenkov telescopes of the TAIGA-IACT installation in the stereo mode.

In the following sections, we describe the configuration of the TAIGA-IACT installation composed of five telescopes, the procedure for modeling hadron and γ-ray events detected by the TAIGA-IACT instal-

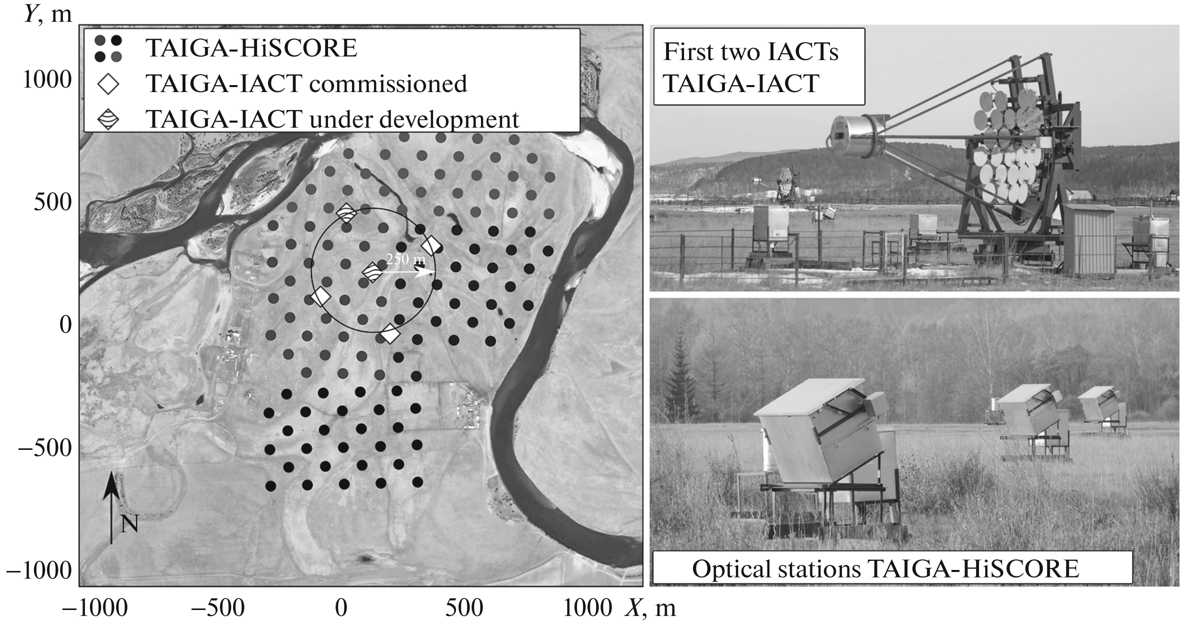

Fig. 1. Relative position of the detectors of the TAIGA astrophysical complex.

lation, and the procedure for analyzing events detected by the installation in the stereo mode.

2. TAIGA-IACT

The imaging atmospheric Cherenkov telescope is equipped with an alt-azimuth mount, which allows tracking of γ-ray sources. The telescope includes a 4.3-m-diameter reflector consisting of 34 spherical mirrors with a diameter of 60 cm, and a detecting camera located at the focus. The viewing angle of the telescope is 9.6° (0.36° per pixel) with point spread function (PSF) of 0.07° [22]. The focal length of the telescopes is 4.75 m. The cameras contain approximately 600 XP1911 photomultiplier tubes (PMTs) with a 15-mm-diameter photocathode. All pixels are grouped into clusters, each of which is controlled by a board based on an MAROC3 application-specific integrated circuit [23]. Each of the 64 MAROC3 channels includes a preamplifier with adjustable gain, a charge-sensitive amplifier with a variable integration time, and a comparator with a configurable threshold. The chip has an analog multiplexed output that is connected to a 12-bit ADC [24].

Each PMT is connected to two MAROC3 channels. The difference in the gain coefficients of the preamplifiers of these channels is 30, which ensures the linearity of the charge-to-code conversion for up to 3000 photoelectrons with a PMT gain of 10^5. A local cluster trigger is generated if the signals of two adjacent PMTs (pixels) in a cluster exceed the threshold amplitude within 15 ns.

The detecting camera of the telescope forms an angular EAS image, the shape of which can be used to reconstruct the parameters of the primary particle, such as the particle type (hadron/γ), energy, direction of arrival, and position of the EAS axis.

According to the observations of the first IACT, γ-ray photons from Markarian 421 blazar were detected in the mono observation mode. The significance of the γ-ray excess was 5σ [25]. The first two telescopes detected γ-rays from the Crab Nebula in both mono [21] and stereo modes at a statistical significance level of 12σ and 5σ, respectively.

3. MONTE CARLO SIMULATION

The EAS simulation was carried out using the CORSIKA program [26] version 7.35 using the QGS-JET-II-04 model [27] for high-energy interactions and GHEISHA-2002d [28] for low-energy interactions. The positions of five TAIGA-IACT telescopes were used in the input files. Showers from primary protons and γ-rays were simulated. The energy range was 40–400 TeV for protons and 20–200 TeV for γ-ray photons with a spectrum slope of −1. The zenith angles of 30°–40° corresponded to the observation of the Crab Nebula in the Tunka Valley. Photons from the CORSIKA output data were tracked in the dedicated TAIGA-optics optical modeling program [29]. This program simulates the optical response of TAIGA atmospheric Cherenkov telescopes up to PMT photocathodes.

The data on the number of photoelectrons in camera pixels obtained on the basis of the optical modeling program were used to simulate the camera response, which included the procedure for generating the telescope trigger (see Section 2). In this case, the photo-

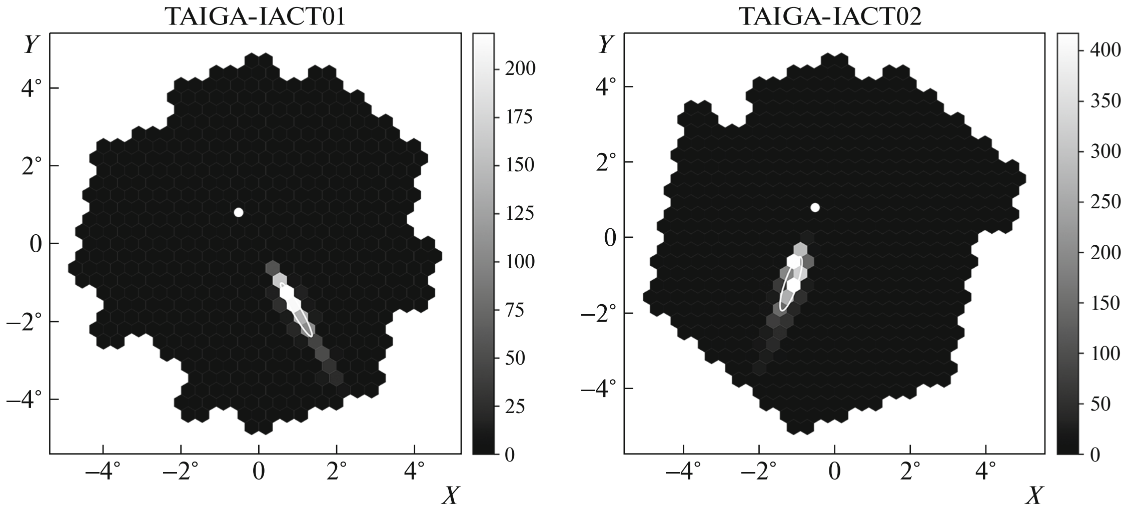

Fig. 2. Example of an event detected by the first two telescopes of the TAIGA-IACT installation. The white dot is the position of the γ-ray source in the field of view of the telescope. The ellipse is an approximation of the EAS image proposed by Hillas [31].

electron amplitudes were randomly selected in accordance with the amplitude distribution measured for XP1911 PMT in [30], which also took into account the influence of afterpulses.

As a result of the described procedure, a set of images generated in the camera of each of the triggered telescopes was obtained for each simulated EAS. Figure 2 shows an example of an event detected by the first and second telescopes of the installation.

Since each pixel of the telescope surveys an individual area of the sky, the distances in the images obtained from the telescope cameras are measured in degrees. The standard analysis of the detected EAS assumes the parameterization of images proposed by Hillas [31]. As a result of the parameterization, each image can be represented by an ellipse, the center of which are the first-order moments (*Xc*, *Yc*), and the axes are the second-order moments (*width*, *length*) of the original image in the detecting camera of the telescope. The following parameters are also calculated for subsequent analysis:

1. *size* - the total number of photoelectrons in the event;

2. *alpha* - the angle between the major axis of the ellipse and the line connecting the center of gravity (CoG) of the image and the position of the source in the field of view of the telescope.

This parameterization allows for an effective analysis of the detected events, as a result of which the main EAS parameters can be reconstructed and γ—hadron separation can be performed.

Since only a part of the installation is often triggered during EAS detection (depending on the energy of the primary particle and the position of the EAS axis), all events can be analyzed in different stereo modes, such as 2, 3, 4, and 5. In other words, the analysis can be performed separately for events detected by only two telescopes, three, etc. In this paper, all calculations are performed for events detected in the 2+ mode, which means that the analysis includes events that triggered two or more telescopes.

In addition to the selection by the number of triggered telescopes, the events recorded in stereo mode were limited by the total number of photoelectrons (more than 120) and the position of the CoG of the ellipse in the camera (less than 3.5°) from the center of the camera. These limitations are related to the fact that dimmer and cropped by the camera edge images, as a rule, impair the accuracy in reconstructing the EAS geometry.

To verify the correspondence between simulation and experimental data, distributions of the total number of photoelectrons were constructed on their basis for events detected by two telescopes (Fig. 3a). The counting rate of such events was approximately ten times lower than that of mono events, both in the simulated samples and in the experiment.

3.1. Reconstructing the Direction of EAS Arrival

When point γ-ray sources are observed, the direction of arrival of EAS from γ-ray photons in the FoV of the telescope is known. Therefore, reconstructing the position of the source can be useful for γ—hadron separation. To solve this problem, the direction of particle arrival was determined as the weighted average position of the intersection points of the major axes for all ellipses (Fig. 4). The axes of the images in the two triggered telescopes intersect at a point

$$x = \frac{b_2 - b_1}{a_1 - a_2} \quad \text{and} \quad y = a_1 x + b_1, \tag{1}$$

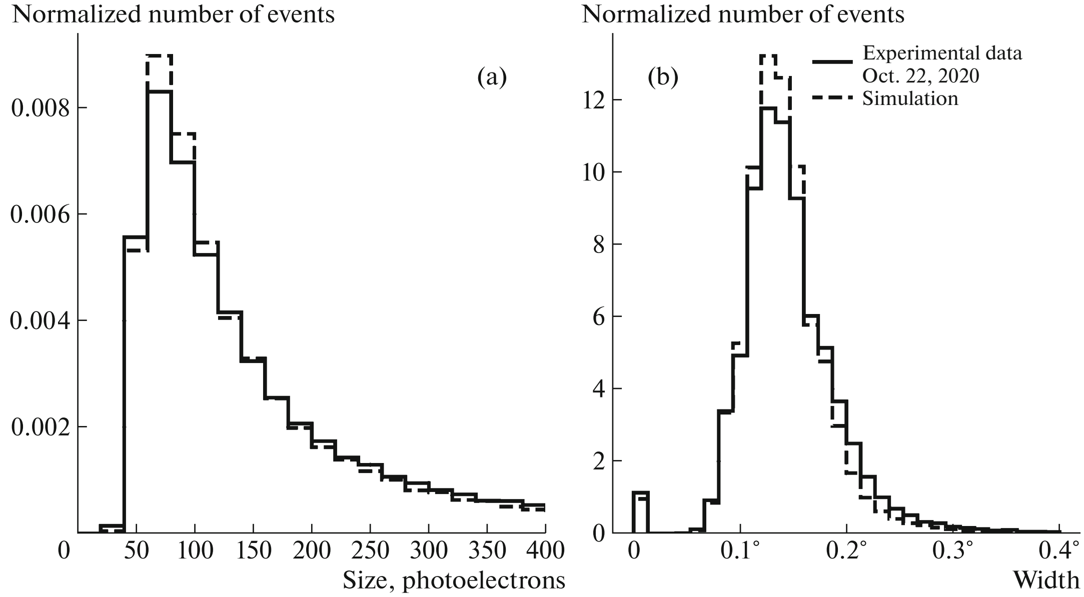

Fig. 3. Comparison of the experimental and Monte Carlo distributions of (a) the *size* events detected by the TAIGA-IACT01 telescope and (b) the *width* events detected by the TAIGA-IACT01 telescope.

where a_i and b_i are the coefficients in the equations for the major axes of ellipses of the form $y = ax + b$. Each pair of telescopes provides a point that falls into a two-dimensional histogram with a weight

$$\frac{size_1 + size_2}{\sum_i^{N_{\text{trig}}} size_i} \sin \Delta, \tag{2}$$

where Δ is the angle between the intersecting lines [10] and N_{trig} is the number of triggered telescopes. The resulting direction of arrival of the event is determined as the mean value of the histogram filled with intersection points

$$x_{\text{mean}} = \frac{1}{N_{\text{bin}}} \sum_i^{N_{\text{bin}}} x_i \quad \text{and} \quad y_{\text{mean}} = \frac{1}{N_{\text{bin}}} \sum_j^{N_{\text{bin}}} y_j, \tag{3}$$

where N_{bin} is the number of bins of the histogram along the axis (the same for x and y). Figure 5a shows the distribution of the error in reconstructing the position of the source in the FoV of the telescope (θ). The mean error was 0.14°. The mean error hereafter refers to the radius of the circle containing 68% of the number of events included in the analysis.

3.2. Reconstructing the Position of the EAS Axis

The EAS axis is reconstructed following the technique that is used to reconstruct the position of the source. In this case, the positions of the triggered telescopes relative to each other, as well as the zenith angle of observation, are taken into account. Figure 5b shows the distribution of the error in reconstructing the position of the EAS axis. The mean error is 24 m.

3.3. Effective Area

To estimate the effective area of the installation and optimize the criteria for the selection of γ-rays, a set of events from primary protons of cosmic rays in the energy range from 40 to 400 TeV was simulated. For all simulated events, the EAS parameters were reconstructed, on the basis of which γ-ray photons were

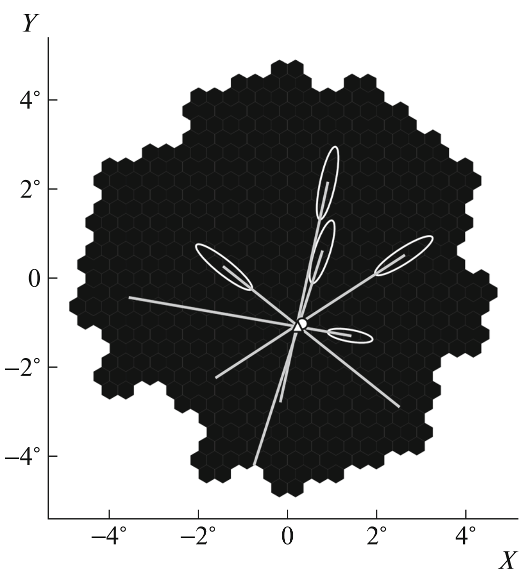

Fig. 4. Determining the position of the source in the FoV of the telescopes. Ellipses are the approximations of the EAS image in each telescope, the intersections of the major axes of which provide the reconstructed position of the source.

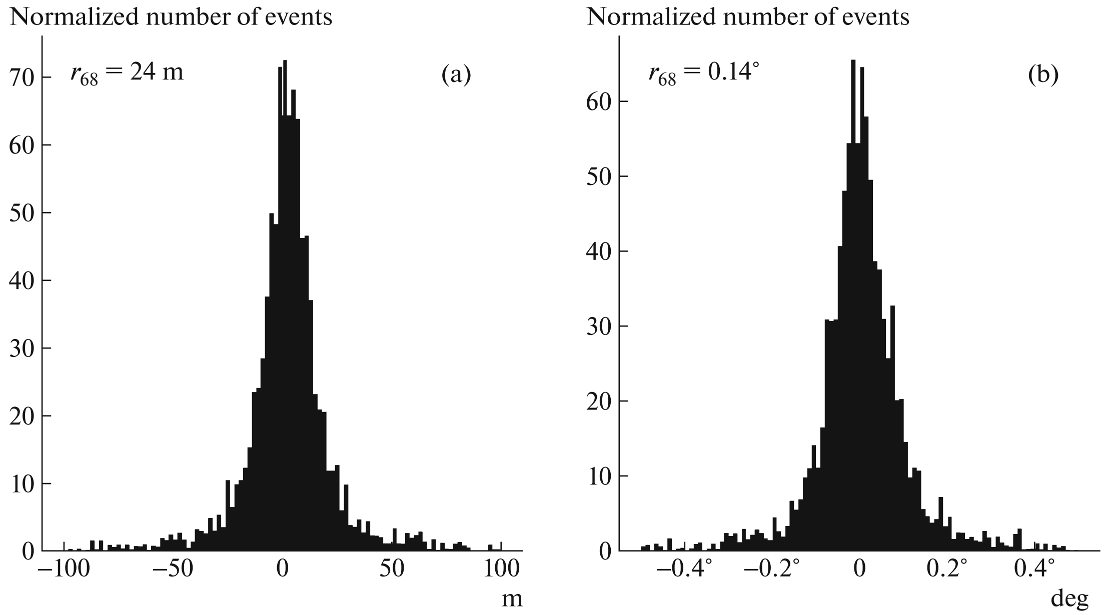

Fig. 5. Error in reconstructing (a) the position of the EAS axis and (b) the direction of EAS arrival.

selected. The selection of γ-rays was carried out by applying the selection criteria to the following event parameters:

1. the square of the angle between the direction of EAS arrival and the direction towards the source under study (θ^2);

2. the normalized width (w).

In the stereoscopic approach, the normalized width is similar to the *width* parameter described in Section 3. It is determined as follows [32]:

$$w = \frac{1}{N_{\mathrm{tel}}}\left[\sum_{i}^{N_{\mathrm{trig}}}\frac{width_i - w_m(r_i, size_i)}{w_{\mathrm{MAD}}(r_i, size_i)}\right], \qquad (4)$$

where N_{tel} is the number of triggered telescopes, $width_i$ is the *width* parameter in this triggered telescope, $w_m(r_i, size_i)$ is the median width value characteristic of events with a given $size_i$ and distance to the shower axis (r_i), $w_{\mathrm{MAD}}(r_i, size_i)$ is the median absolute deviation of the *width* parameter distribution for events in the same range of values of r_i and $size_i$, and w_{MAD} and w_m are the tabular values and are determined from the simulation.

Based on the obtained dependences for w_{MAD} and w_m on the total number of photoelectrons, a distribution of normalized widths was obtained in accordance with Eq. (4) for simulated γ-ray photons and hadrons (Fig. 6).

The optimal criteria for the selection of γ-rays were determined via optimization, in which a limitation was placed on each of the three parameters described above, the value of which varied from the minimum to maximum value of this parameter. During the optimization, all possible combinations of selection criteria were tested. A combination was found in which the proportion of saved γ-ray photons remained at a level of 50% of the number of events detected in stereo mode, and the suppression of hadrons turned out to be maximum. The resulting suppression of hadrons was on the order of 4.2×10^{-5}.

The effective area of the TAIGA-IACT installation was constructed based on the obtained event-selection criteria (Fig. 7). In the energy range above 30 TeV, the effective area exceeds 0.5 km^2. As a result, 1225, 132, and 48 γ-ray photons can be detected over 200-h observation from the Crab Nebula, the CTA1 pulsar wind nebula, and the Tycho supernova remnant, respectively.

3.4. Energy Reconstruction

The energy of detectable EAS initiated by γ-rays is currently reconstructed on the basis of three parameters:

1. *size*;

2. the distance to the EAS axis;

3. the maximum depth of shower development $X_{\max}$.

3.4.1. Reconstruction of the maximum depth of EAS development. $X_{\max}$ can be reconstructed if the height of the EAS development maximum is known. For stereo systems of Cherenkov telescopes, there is a technique that allows one to determine this parameter.

This technique is based on the fact that the EAS image in the telescope camera contains information about the angle between the direction of EAS arrival and the direction towards the maximum of EAS devel-

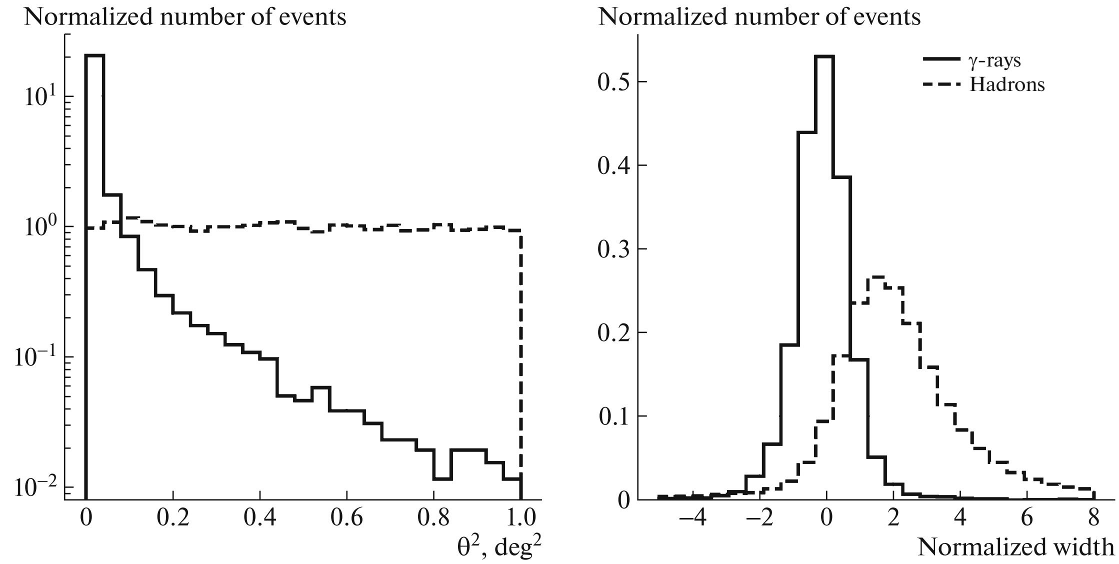

Fig. 6. Distributions of parameters θ^2 and the normalized width of the simulated events from primary γ-rays and hadrons detected by the TAIGA-IACT telescopes.

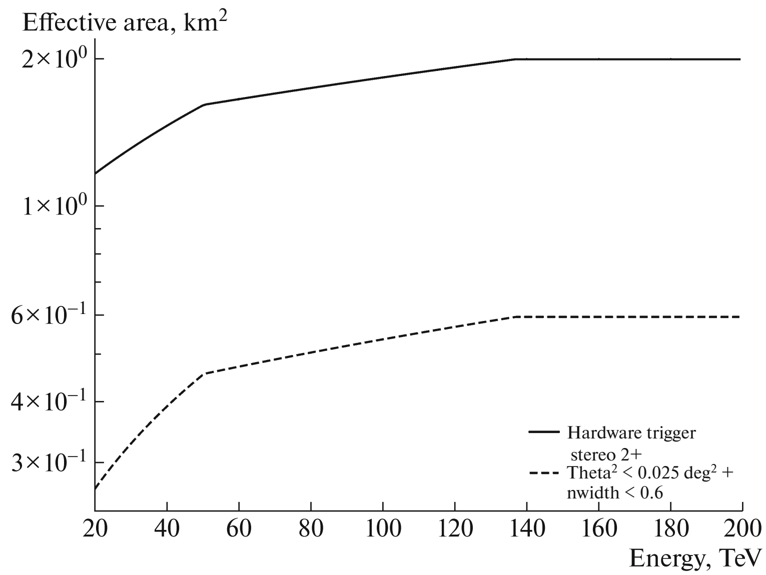

Fig. 7. Effective area of the TAIGA-IACT installation after modeling the hardware trigger of telescopes and applying optimal criteria for selecting γ-like events.

opment. The shower development maximum corresponds to the CoG of the image and, knowing the distance to the axis, one can calculate the height of the shower development maximum from the geometry [33]:

$$height = \frac{impact}{dist}, \tag{5}$$

where *impact* is the distance between the telescope and the EAS axis and *dist* is the angle between the direction towards the source and the center of gravity of the image. The altitude can be transformed to g/cm^2 units using a standard atmosphere model for an altitude of 450 m above sea level and an average temperature of −17.5°C [34].

The mean value of the $X_{\max}$ reconstruction error calculated according to Eq. (5) changes with an increase in the distance towards the EAS axis from 90 to −120 g/cm^2. This is due to the fact that the CoG position of the image does not exactly correspond to

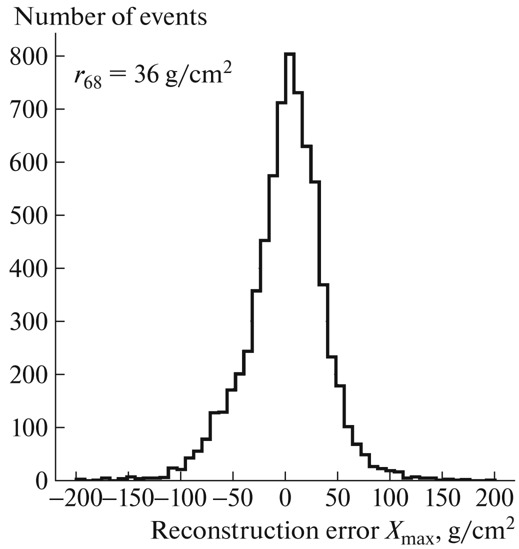

Fig. 8. Error in reconstructing the depth of the maximum of EAS development.

the EAS development maximum. At small distances to the axis (up to 400 m), the *dist* value for determining the height of the shower development maximum is underestimated. Above 400 m, the *dist* value overestimates the evaluated value of the X_{max} position. The dependence of the average error of the reconstructed X_{max} values on the distance to the axis can be corrected by the linear function. In our case:

$$d_{X_{\max}} = a \times impact + b, \tag{6}$$

where $a = -0.14$, $b = 58.15$, and $d_{X_{\max}}$ is the surplus factor. The use of this dependence to correct the reconstructed value of the maximum height of the EAS development has led to a decrease in the mean error to 36 g/cm^2 (Fig. 8).

3.4.2. Energy spectrum and resolution. In order to reconstruct the energy of individual events, the dependence of the particle energy on the total number of photoelectrons of the image recorded by the telescope in the simulation was determined. This dependence appears to be different for different X_{max} values and distances to the axis in each individual event.

In this regard, the entire space of possible X_{max} values and distances to the axis was divided into separate bins with step of 72 g/cm^2 and 10 m, respectively. For events that fell into a certain X_{max} and *distance* bin, linear dependences of the energy on the *size* were determined, on the basis of which the reconstructed energy could be obtained. The energy resolution was calculated for each energy bin using the formula

$$E_{\rm res} = \frac{1}{N}\sum_{i}^{N}\frac{\left|E_i^{\rm reco} - E_i^{\rm sim}\right|}{E_i^{\rm sim}}, \tag{7}$$

where N is the number of events in a certain energy bin, $E_i^{\rm reco}$ is the reconstructed energy of the event, and $E_i^{\rm sim}$ is the simulated energy of the event. This method was applied to the reconstruction of event energies in the range of 20–200 TeV, and the energy resolution was approximately 10% (Fig. 9).

4. CONCLUSIONS

The paper presents the possibilities of determining the parameters of γ-rays with energies of 20–200 TeV detected by the TAIGA-IACT installation consisting of five telescopes. The error in determining the position of the source was 0.14°, and the position of the EAS axis is reconstructed with an accuracy of 24 m. The position of the maximum of the shower development can be determined with an accuracy of 36 g/cm^2, which leads to an energy resolution of the reconstructed γ-ray spectrum at a level of approximately 10%. The suppression of the hadron background is on

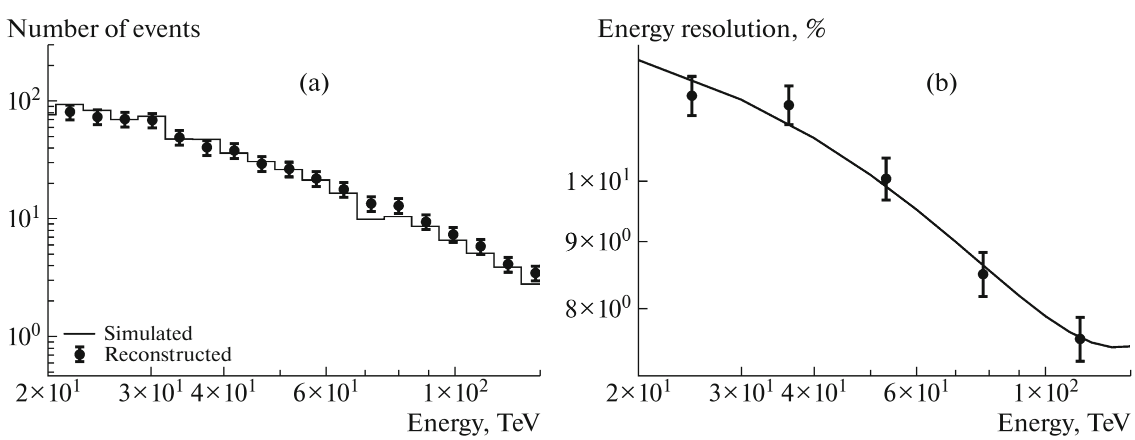

Fig. 9. (a) Reconstructed and simulated energy spectrum of simulated γ quanta and (b) the energy resolution.

the order of 4.2×10^{-5} at an effective installation area of 0.6 km^2 in the energy region above 30 TeV. This will allow acquisition of significant statistics in 200-h observations of the Crab Nebula, the pulsar wind nebula in CTA1, and the Tycho supernova remnant: 1225, 132, and 48 events, respectively.

FUNDING

This study was carried out at the Unique Scientific Facility Astrophysical Complex of Moscow State University and Irkutsk State University under support of the Ministry of Education and Science of the Russian Federation (agreement EV-075-15-2021-675) and the Russian Science Foundation (project no. 23-72-00019, sections 3, 4) as well as in the context of state assignments (FZZE-2020-0017, FZZE-2020-0024, FSUS-2020-0039).

CONFLICT OF INTEREST

The authors of this work declare that they have no conflicts of interest.

REFERENCES

1. Amenomori, M., Bao, Y.W., Bi, X.J., Chen, D., Chen, T.L., Chen, W.Y., Chen Xu, Chen, Y., Cirennima, Cui, S.W., Danzengluobu, Ding, L.K., Fang, H., Fang, K., Feng, C.F., et al., *Phys. Rev. Lett.,* 2019, vol. 123, p. 051101. https://doi.org/10.1103/PhysRevLett.123.051101
2. Cao, Z., Aharonian, F.A., An, Q., Axikegu, L.X., Bai, L.X., Bai, Y.X., Bao, Y.W., Bastieri, D., Bi, X.J., Bi, Y.J., Cai, H., Cai, J.T., Zhe Cao, Chang, J., Chang, F., et al., *Nature,* 2021, vol. 594, p. 33. https://doi.org/10.1038/s41586-021-03498-z
3. Liu, R.-Y. and Wang, X.-Y., *Astrophys. J.,* 2021, vol. 922, p. 221. https://doi.org/10.3847/1538-4357/ac2ba0
4. Abeysekara, A.U., Albert, A., Alfaro, R., Angeles Camacho, J.R., Arteaga-Velázquez, J.C., Arunbabu, K.P., Avila Rojas, D., Ayala Solares, H.A., Baghmanyan, V., Belmont-Moreno, E., BenZvi, S.Y., Brisbois, C., Caballero-Mora, K.S., Capistrán, T., Carramiñana, A., et al., *Phys. Rev. Lett.,* 2020, vol. 124, p. 021102. https://doi.org/10.1103/PhysRevLett.124.021102
5. Budnev, N., Chernov, D., Gress, O., Korosteleva, E., Kuzmichev, L., Lubsandorzhiev, B., Navarra, G., Pankov, L., Prosin, V., Semeney Yu., et al., *Astropart. Phys.,* 2013, vols. 50–52, p. 18. https://doi.org/10.1016/j.astropartphys.2013.09.006
6. Berezhnev, S.F., Besson, D., Budnev, N.M., Chiavassa, A., Chvalaev, O.A., Gress, O.A., Dyachok, A.N., Epimakhov, S.N., Haungs, A., Karpov, N.I., Kalmykov, N.N., Konstantinov, E.N., Korobchenko, A.V., Korosteleva, E.E., Kozhin, V.A., et al., *Nucl. Instrum. Methods Phys. Res., Sect. A,* 2012, vol. 692, p. 98. https://doi.org/10.1016%2Fj.nima.2011.12.091
7. Apel, W.D., Arteaga-Velázquez, J.C., Bekk, K., Bertaina, M., Blümer, J., Bozdog, H., Brancus, I.M., Buchholz, P., Cantoni, E., Chiavassa, A., Cossavella, F., Daumiller, K., de Souza, V., Di Pierro, F., Doll, P., et al., *Astropart. Phys.,* 2012, vol. 36, no. 1, p. 183. https://doi.org/10.1016/j.astropartphys.2012.05.023
8. Monkhoev, R.D., Budnev, N.M., Chiavassa, A., Dyachok, A.N., Gafarov, A.R., Gress, O.A., Gress, T.I., Grishin, O.G., Ivanova, A.L., Kalmykov, N.N., Kazarina Yu.A., Korosteleva, E.E., Kozhin, V.A., Kuzmichev, L.A., Lenok, V.V., et al., *J. Instrum.,* 2017, vol. 12, p. C06019. https://doi.org/10.1088/1748-0221/12/06/c06019
9. Fedorov, O., Bezyazeekov, P.A., Budnev, N.M., Chernykh, D., Gress, O.A., Haungs, A., Hiller, R., Huege, T., Kazarina, Y., Kleifges, M., Korosteleva, E.E., Kostunin, D., Krömer, O., Kuzmichev, L.A., Lenok, V., et al., arXiv:1712.00974v1 [astro-ph.IM], 2017. https://doi.org/10.48550/ARXIV.1712.00974
10. Yashin, I.I., Astapov, I.I., Barbashina, N.S., Bogdanov, A.G., Boreyko, V., Budnev, N.M., Büker, M., Bruckner, M., Chiavassa, A., Chvalaev, O.B., Gafarov, A.V., Gorbunov, N., Grebenyuk, V., Gress, O.A., Grinyuk, A., et al., *J. Phys.: Conf. Ser.,* 2016, vol. 675, no. 3, p. 032037. https://doi.org/10.1088/1742-6596/675/3/032037
11. Tluczykont, M., Hampf, D., Horns, D., Spitschan, D., Kuzmichev, L., Prosin, V., Spiering, C., and Wischnewski, R., *Astropart. Phys.,* 2014, vol. 56, p. 42. https://www.sciencedirect.com/science/article/pii/S0927650514000322. https://doi.org/10.1016/j.astropartphys.2014.03
12. Kuzmichev, L., Astapov, I., Bezyazeekov, P., Boreyko, V., Borodin, A., Brückner, M., Budnev, N., Chiavassa, A., Gress, O., Gress, T., Grishin, O., Dyachok, A., Epimakhov, S., Fedorov, O., et al., *EPJ Web Conf.,* 2017, vol. 145, p. 01001. https://doi.org/10.1051/epjconf/201714501001
13. Tluczykont, M., Budnev, N., Astapov, I., Barbashina, N., Bogdanov, A., Boreyko, Brückner, M., Chiavassa, A., Chvalaev, O., Gress, O., Gress, T., Grishin, O., Dyachok, A., Epimakhov, S., Fedorov, O., et al., *EPJ Web Conf.,* 2017, vol. 136, p. 03008. https://doi.org/10.1051/epjconf/201713603008
14. Hinton, J.A., *New Astron. Rev.,* 2004, vol. 48, nos. 5–6, p. 331. https://doi.org/10.1016/j.newar.2003.12.004
15. Cortina, J., *Proc. 32nd Int. Cosmic Ray Conference,* Beijing, 2011, vol. 11, p. 147. https://doi.org/10.48550/arXiv.1110.4747
16. Perkins, J.-S., Maier, G., VERITAS Collab., *Proc. Fermi Symposium,* Washington, DC, 2009. arXiv:0912.3841 [astro-ph.IM]. arXiv:0912.3841v1 [astro-ph.IM.]. https://doi.org/10.48550/arXiv.0912.3841
17. Acharya, B.S., Actis, M., Aghajani, T., Agnetta, G., Aguilar, J., Aharonian, F., Ajello, M., Akhperjanian, A., Alcubierre, M., et al., *Astropart. Phys.,* 2013, vol. 43, p. 3. https://doi.org/10.1016/j.astropartphys.2013.01.007
18. Brown, A.M., Acharyya, A., Dominguez, A., Hassan, T., Lenain, J.-P., and Pita, S., *Proc. Sci.,* 2021, vol. 395, p. 0887. https://doi.org/10.22323/1.395.0887

19. Archambault, S., Archer, A., Benbow, W., Bird, R., Bourbeau, E., Buchovecky, M., Buckley, J.H., Bugaev, V., Cerruti, M., Connolly, M.P., Cui, W., Dwarkadas, V.V., Errando, M., Falcone, A., Feng, Q., et al., *Astrophys. J.,* 2017, vol. 836, no. 1, p. 23. https://doi.org/10.3847/1538-4357/836/1/23
20. Aliu, E., Archambault, S., Arlen, T., Aune, T., Beilicke, M., Benbow, W., Bouvier, A., Buckley, J.H., Bugaev, V., Cesarini, A., Ciupik, L., Collins-Hughes, E., Connolly, M.P., Cui, W., Dickherber, R., et al., *Astrophys. J.,* 2013, vol. 764, no. 1, p. 38. https://doi.org/10.1088/0004-637X/764/1/38
21. Sveshnikova, L.G., Volchugov, P.A., Postnikov, E.B., Astapov, I.I., Bez"yazykov, P.A., Bonvech, E.A., Borodin, A.N., Budnev, N.M., Bulan, A.V., Vaidyanatan, A., Volkov, N.V., Voronin, D.M., Gafarov, A.R., Gres', E.O., Gres', O.A., et al., *Bull. Rus. Acad. Sci.: Phys.,* 2023, vol. 87, no. 7, p. 904. https://doi.org/10.3103/S1062873823702738
22. Kuzmichev, L., Astapov, I., Bezyazeekov, P., Borodin, A., Brückner, M., Budnev, N., Chiavassa, A., Gress, O., Gress, T., Grishin, O., Dyachok, A., Fedorov, O., Gafarov, A., Garmash, A., Grebenyuk, V., et al., *Nucl. Instrum. Methods Phys. Res., Sect. A,* 2020, vol. 952, p. 161830. https://doi.org/10.1016/j.nima.2019.01.056
23. Kompaniets, K.G., TAIGA Collab., *Proc. Int. Symposium on Cosmic Rays and Astrophysics (ISCRA2019),* Moscow, 2019. https://iscra2019.mephi.ru/content/public/files/posters/Poster_4_07_KompanietsK.pdf.
24. Lubsandorzhiev, N., Astapov, I., Bezyazeekov, P., Boreyko, V., Borodin, A., Brückner, M., Budnev, N., Chiavassa, A., Dyachok, A., Fedorov, O., Gafarov, A., Garmash, A., Gorbunov, N., Grebenyuk, V., Gress, O., et al., *Proc. Sci.,* 2017, vol. 301, p. 0757. https://doi.org/10.22323/1.301.0757
25. Sveshnikova, L., Astapov, I., Bezyazeekov, P., Blank, M., Borodin, A., Brückner, M., Budnev, N., Bulan, A., Neelakandaiyer, A., Wischnewski, R., Volchugov, P., Voronin, D., Gafarov, A., Garmash, A., Grebenyuk, V., et al., *Bull. Rus. Acad. Sci.: Phys.,* 2021, vol. 85, p. 398. https://doi.org/10.3103/S1062873821040365
26. Heck, D., Knapp, J., Capdevielle, J.N., Schatz, G., and Thouw, T., *Technical Report FZKA-6019,* Karlsruhe: Forschungszentrum Karlsruhe, 1998. https://doi.org/10.5445/IR/270043064
27. Ostapchenko, S., *Phys. Rev. D,* 2011, vol. 83, no. 1, p. 014018. https://doi.org/10.1103/PhysRevD.83.014018
28. Fesefeldt, H., *The Simulation of Hadronic Showers: Physics and Applications, Technical Report,* Aachen: Physikalisches Institut, Technische Hochschule Aachen (PITHA), 1985. http://cds.cern.ch/record/162911/files/CM-P00055931.pdf.
29. Grinyuk, E., Postnikov, N., and Sveshnikova, L., *Phys. At. Nucl.,* 2020, vol. 83, p. 262. https://doi.org/10.1134/S106377882002012X
30. Mirzoyan, R., Lorenz, E., Petry, D., and Prosch, C., *Nucl. Instrum. Methods Phys. Res., Sect. A,* 1997, vol. 387, no. 1, p. 74. https://doi.org/10.1016/S0168-9002(96)00964-3
31. Hillas, A.M., *Proc. 19th Int. Cosmic Ray Conference (ICRC19),* San Diego, CA, 1985, vol. 3, p. 445.
32. Krawczynski, H., Carter-Lewis, D.A., Duke, C., Holder, J., Maier, G., Le Bohec, S., and Sembroski, G., *Astropart. Phys.,* 2006, vol. 25, p. 380. https://doi.org/10.1016/j.astropartphys.2006.03.011
33. Hofmann, W., Lampeitl, H., Konopelko, A., and Krawczynski, H., *Astropart. Phys.,* 2000, vol. 12, no. 4, p. 207. https://doi.org/10.1016%2Fs0927-6505%2899%2900109-7
34. Prosin, V.V., *Doctoral Sci. (Phys.-Math.) Dissertation,* Moscow: Moscow State Univ., 2006.

Translated by N. Goryacheva